



An integrated model of *FTO* and *METTL3* expression that predicts prognosis in lung squamous cell carcinoma patients

Kun Zhang^{1#}, Zhaojie Han^{2#}, Hongmei Zhao³, Siyao Liu³, Fuchun Zeng¹

¹Department of Thoracic Surgery, Sichuan Provincial People's Hospital, Chengdu, China; ²Department of Thoracic Surgery, Southwest Hospital, Army Medical University, Chongqing, China; ³Chosen Med Technology (Beijing) Co., Ltd., Beijing, China

Contributions: (I) Conception and design: F Zeng; (II) Administrative support: K Zhang; (III) Provision of study materials or patients: Z Han; (IV) Collection and assembly of data: H Zhao, S Liu; (V) Data analysis and interpretation: H Zhao, S Liu; (VI) Manuscript writing: All authors; (VII) Final approval of manuscript: All authors.

[#]These authors contributed equally to this work.

Correspondence to: Fuchun Zeng, Department of Thoracic Surgery, Sichuan Provincial People's Hospital, Chengdu 610031, China.

Email: 870239259@qq.com.

Background: Lung squamous cell carcinoma (LUSC) approximately accounts for a third of lung cancers. However, the role of N6-methyladenosine (m6A) in LUSC remains largely unknown according to previous studies.

Methods: In this study, we investigated the mutations, copy number variants (CNVs), expression of 20 m6A RNA methylation regulators, and clinical data from The Cancer Genome Atlas-LUSC (TCGA-LUSC). These data were used for the training cohort of screening potential biomarkers. The prognostic model of m6A RNA methylation regulators was constructed. A receiver operating characteristic (ROC) analysis was undertaken to determine the area under the curves (AUCs) (for 3- and 5-year survival) for the model. Additionally, the accuracy of the two-gene model was confirmed with external data verifications. Combined two-gene model and clinical information were performed to construct a nomogram to predict patient's prognostic risk assessment.

Results: Fat mass- and obesity-associated protein (*FTO*) and methyltransferase-like 3 (*METTL3*) were identified as potential prognostic biomarkers to evaluate benign and malignant tumors and prognosticate. The following prognostic model of m6A RNA methylation regulators was constructed: risk score = $0.162 \times FTO - 0.069 \times METTL3$. Patients in low-risk group [median overall survival (mOS), 43.4 months] had longer survival than those with high-risk (mOS, 67.3 months) with $P=0.0023$. The smoking grade and risk score could be independent prognostic factors ($P=0.00098$ and $P=0.0014$, respectively). Ultimately, a nomogram was developed to assist clinicians to predict clinical outcomes.

Conclusions: *FTO* and *METTL3* are potential prognostic biomarkers of LUSC. The two-gene model's use of prognostic risk scores may provide guidance in the selection of therapeutic strategies.

Keywords: Fat mass- and obesity-associated protein (*FTO*); methyltransferase-like 3 (*METTL3*); N6-methyladenosine (m6A); biomarkers; lung squamous cell carcinoma (LUSC)

Submitted Jul 16, 2021. Accepted for publication Oct 02, 2021.

doi: 10.21037/atm-21-4470

View this article at: <https://dx.doi.org/10.21037/atm-21-4470>

Introduction

About 30% of non-small cell lung cancer is lung squamous cell carcinoma (LUSC) (1). The 5-year survival rate and the prognosis of the disease is closely related to the stage; stage IV has a 5-year rate of only 2% while stage I (no metastasis) has a survival rate of 70% (2,3). Thus, the early diagnosis is extremely important in LUSC. As N6-methyladenosine (m6A) is the most prevalent messenger RNA (mRNA) modification, it plays a key role in physiological and pathological processes (4,5). As previously reported, the role of m6A in the clinical diagnosis and treatment prediction performance of lung adenocarcinoma (LUAD) has been increasingly attended (6-8). However, the effect of m6A RNA modification in LUSC remains unclear, especially in relation to prognostic stratification.

In this study, a survival analysis was conducted and multi-omics were identified to screen potential biomarkers in LUSC. Ultimately, the training cohort comprised 504 patients from The Cancer Genome Atlas (TCGA), and a two-gene model of risk score and prognostic nomogram was built to assist clinicians to make individualized clinical decisions (see *Figure 1*). We present the following article in accordance with the TRIPOD reporting checklist (available at <https://dx.doi.org/10.21037/atm-21-4470>).

Methods

Participants

20 widely acknowledged m6A RNA methylation regulators were arranged from previous studies. Methyltransferase “writers” include *KIAA1429*, *METTL14*, *METTL3*, *RBM15*, *WTAP*, and *ZC3H13*. “Readers”, such as *HNRNPC*, *RBMX*, *HNRNPA2B1*, *YTHDC1*, *YTHDC2*, *YTHDF1*, *YTHDF2*, *YTHDF3*, *FMR1*, *IGF2BP1*, *IGF2BP2*, and *IGF2BP3*, are involved in RNA processing. “Erasers”, such as *ALKBH5* and fat mass- and obesity-associated protein (*FTO*), are involved demethylation modification (9-12). In this study, we examined their role in the prognosis of LUSC in both a training cohort and a validation cohort.

The mutational profiles and copy number variants (CNVs) of 20 m6A RNA methylation regulators were downloaded from TCGA database. We processed and normalized TCGA level 3 RNA-sequencing (RNA-seq) data, and the fragments per kilobase million (FPKM) values of the exon model from TCGA were used for the gene expression levels. The clinical information of 504 LUSC patients was obtained. The RNA-seq data that was

used as the training cohort comprised 504 tumor samples and 49 normal samples. The validation data for *FTO* and methyltransferase-like 3 (*METTL3*) expression were obtained from GSE157009 and GSE157010 in the Gene Expression Omnibus (GEO) (<http://www.ncbi.nlm.nih.gov/geo/>) database. Total RNA data based on GPL570 platforms from squamous cell carcinoma specimens, comprising 249 and 235 patients, were extracted for mRNA profiling and a microarray analysis. The validation data for LUAD were also downloaded from TCGA. To confirm the accuracy of the prognostic model, any patient with missing clinical data was excluded from the training and validation cohorts. The study was conducted in accordance with the Declaration of Helsinki (as revised in 2013).

Differential expression of m6A RNA methylation regulators in LUSC

A comparison of the expression of 19 m6A RNA methylation regulators, excluding *RBMX*, in the TCGA-LUSC using the “limma” package was performed to identify differentially expressed genes (DEGs) in the 504 tumor samples and 49 normal samples. A cutoff value ($P < 0.05$ and $|\log_2FC| > 1$) was used to select DEGs for mRNA expression. Ultimately, 14 of these genes were identified as DEGs.

Mutation and CNV analysis

The genetic alterations of 20 m6A genes in LUSC were explored in 42 patients with single nucleotide variants (SNVs) and 124 patients with CNVs. We divided the 42 patients into two groups based on each mutational and non-mutational gene. The results of the univariate analysis showed that none of the genes with mutations had any significant relationship with prognosis; however, this was because there were few patients with mutations in each group. A profile of the somatic copy number alteration by GISTIC 2.0 showed that 14q.11.2 was significantly amplified in LUSC patients with *METTL3* genes found in a “wide peak” region.

To date, no research appears to have been conducted on whether the high expression of *METTL3* is related to CNVs in LUSC; however, the mRNA expression of *METTL3* has been shown to be positively correlated with the CNVs in liver hepatocellular carcinoma patients and cancer cell lines (13). We performed Wilcoxon rank-sum tests to analyze CNVs in LUSC, and found that increases in CNVs are correlated with the high expression of

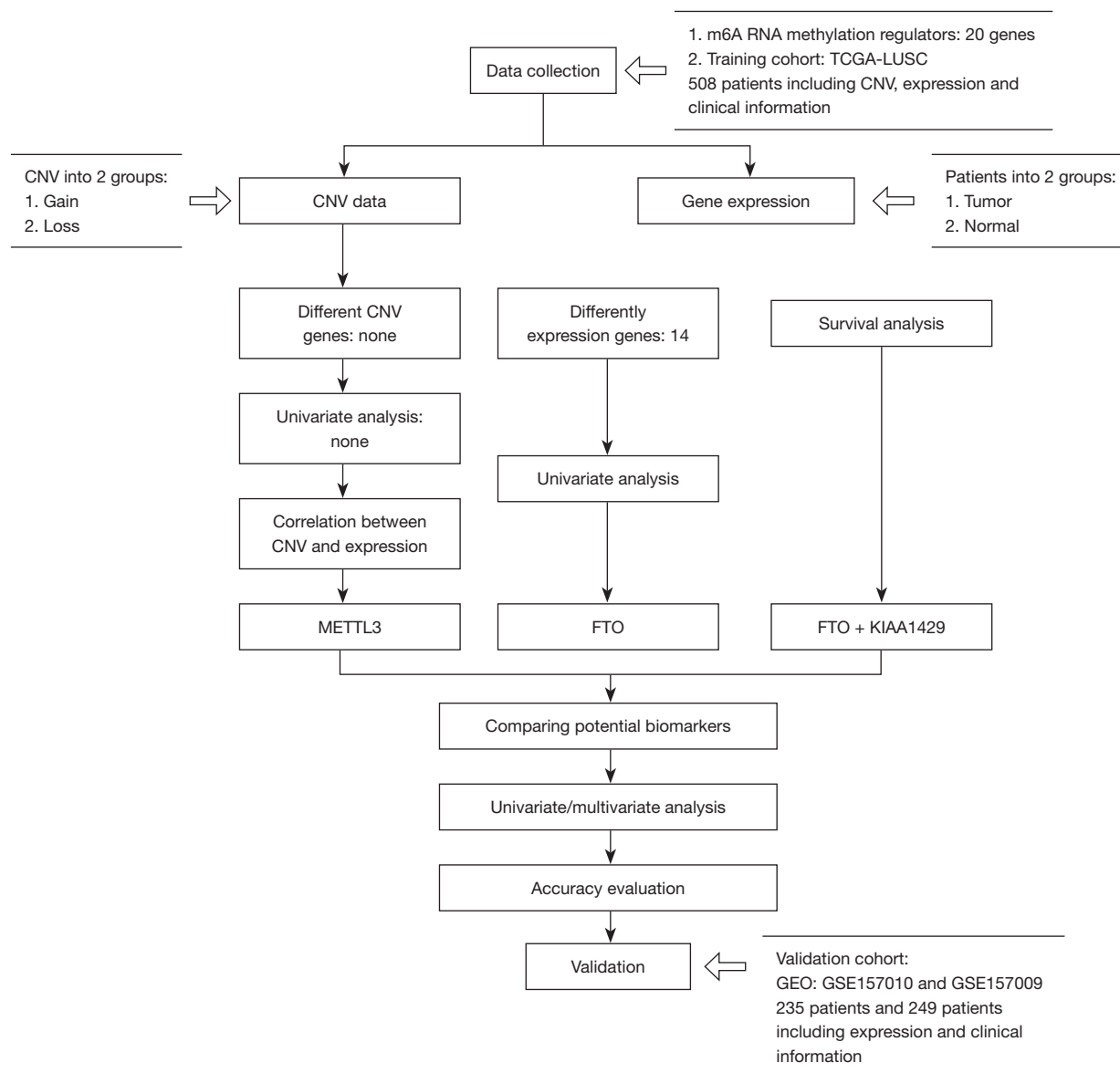


Figure 1 The workflow analysis of a significant prognostic model. m6A, N6-methyladenosine; TCGA, The Cancer Genome Atlas; LUSC, lung squamous cell carcinoma; CNV, copy number variant; GEO, Gene Expression Omnibus.

METTL3 (P<0.01).

of *FTO* and *METTL3*.

Protein-protein interaction (PPI) network analysis of *FTO* and *METTL3*

PPI networks were integrated using the Search Tool for the Retrieval of Interacting Genes (STRING) database (<https://string-db.org>). Cytoscape software (<https://cytoscape.org>) was used to establish and visualize the interaction network

Survival analysis

We sought to examine correlations between genetic alterations and the expression of m6A RNA methylation regulators and prognosis. First, we used the Cox proportional hazards model and R package “survival” and “survminer” to analyze 20 m6A RNA methylation regulators on CNV.

The CNV group was divided into gain and loss groups, and Kaplan-Meier curves were generated for each gene. The results revealed that none of the 20 m6A RNA methylation regulators based on CNV were significantly related to prognosis. Next, 20 m6A RNA methylation regulators on expression were screened using the same method outlined above. An analysis of 14 DEGs in relation to the overall survival (OS) curves showed that *FTO* (P=0.041) and *KIAA1429* (P=0.034) were potential prognostic genes (see Figure S1A,S1B).

Risk scores of m6A RNA methylation regulators

Based on the results of the expression and univariate Cox regression analyses, we built a two-gene model of *FTO* and *KIAA1429* to predict prognostic values according to a survival analysis. The minimum criteria determined the regression coefficients. The prognostic risk score of the biomarkers was calculated using the following formula:

$$\text{Risk score} = \sum_{i=1}^n \text{Coef}_i \times X_i \quad [1]$$

where Coef_i is the regression coefficient and X_i is the expression of each selected m6A RNA methylation regulator. Based on the coefficients and the minimum criteria of two selected m6A RNA methylation regulators, the regression coefficients were 0.162 and 0.163, respectively. Finally, the two-gene model was constructed to be a prognostic model (P=0.012) as Model-1, which states:

$$\text{Risk score} = 0.162 \times \text{FTO} + 0.163 \times \text{KIAA1249} \quad [2]$$

To assess the prediction precision of the prognostic risk-score model, we used a receiver operating characteristic (ROC) curve and calculated the area under the curve (AUC) for 5 years survival (AUC =0.547). The accuracy of *FTO* and *KIAA1249* expression was not satisfactory for prognosis.

Comparing with a biomarker *KIAA1249*, we took *METTL3* into account with *FTO* expression forming a complex two-gene model. Thus, *METTL3* was accepted as a risky gene for evaluating the risk score of the LUSC patients. Integrating two biomarkers into one prognostic risk model could improve the prediction performance of the model.

To investigate the prognostic risk score of the two-gene model, we separated 504 patients from the TCGA-LUSC database into low- and high-risk groups based on median risk scores. The regression coefficients based on the minimum criteria and the coefficients of the two selected m6A RNA methylation regulators were 0.162 and -0.069,

respectively. A two-gene model was then constructed to be a prognostic risk-score model (P=0.0023). Model-2 states:

$$\text{Risk score} = 0.162 \times \text{FTO} - 0.069 \times \text{METTL3} \quad [3]$$

The risk score showed good prediction efficiency with areas under the ROC curve for 3- and 5-year survival in the training cohort of 0.627 and 0.653, respectively, which were higher than those of the *FTO* and *KIAA1429* model and were associated with each other in the PPI network.

As well known, *FTO* as “erasers” are involved in m6A demethylase modification and *METTL3* as “writers” are involved in m6A methylase modification. High *FTO* expression was associated with a poor prognosis, but high *METTL3* expression with associated with a good prognosis. Additionally, as the above study showed, *FTO* was negatively correlated with *METTL3* (P<0.0001). A differential expression analysis showed that *FTO* was expressed at a significantly low level in tumor samples, but at a high level in normal samples. Conversely, *METTL3*, a m6A methylase, was not significantly more upregulated relative to normal controls (P>0.05).

Verifying the accuracy of the prognostic model in validation cohort

The prognostic risk-score model was further validated in the independent GSE157010 using the GEO database as the validation cohort. The two-gene model was verified on 235 patients with LUSC from the validation cohort I. A survival analysis was performed, and the AUC was used to evaluate sensitivity and specificity. In order to obtain independent verification, validation cohort II (GSE157009) including 249 patients) was considered into the two-gene model.

Further, the diagnostic risk scores of the two-gene model could be used to diagnose LUAD (mOS: 58.4 months; AUC: 0.54; P<0.05); however, these results were not significant than those for LUSC. Thus, the prognostic risk scores enabled clinicians to predict outcomes for LUSC, but not LUAD. To determine the reason for these different results, *FTO* and *METTL3* expression in LUSC were compared to those in LUAD. There was no significant difference in *FTO* expression (P=0.7644) between LUSC and LUAD, but the difference in *METTL3* expression in LUSC and LUAD were strong and significantly different (P=0.003629). Specifically, a Wilcox test showed that *METTL3* expression was higher in LUAD than in LUSC. Thus, *METTL3* could have different regulatory mechanisms

in LUSC and LUAD.

Statistical analysis

The ‘limma’ package (<http://bioinf.wehi.edu.au/limma>) was used to identify DEGs in the tumor and normal groups (cutoff: $P < 0.05$ and $|\log_2FC| > 1$). A Spearman correlation analysis was undertaken to examine correlations in gene expression. Wilcoxon rank-sum tests were performed to examine the relationship between CNVs and gene expression. PPI networks were visualized based on the STRING database (<https://string-db.org>). Univariate and multivariate Cox regression analyses were conducted to evaluate the association between variables with OS in the ‘survival’ R package. The log-rank test was used to compare prognostic values. In this study, the AUC was used as the performance measurement method for the predictive models. AUC was plotted using the ‘survivalROC’ R package. The logistic regression model was built to diagnose in early patients. Using the Cox regression model, the prognostic nomogram for OS was constructed using “regplot” R package, and all statistical tests were performed using R-3.6.3.

Results

Participants

The clinical information of 504 patients in the training cohort was put in order and the clinicopathological features [e.g., age, gender, tumor, node and metastasis (TNM) status, T status, N status, M status and smoking grade] were selected as potential prognostic factors. To confirm the accuracy of the prognostic model, any patient with missing clinical data in the training cohort was excluded, and validation cohort I (235 patients) and validation cohort II (249 patients) were performed to verify the accuracy of the prognostic model, respectively (see [Table 1](#)).

Differential expression and co-expression in LUSC

We found that 14 genes showed significant differential expression (cutoff of $P < 0.05$ and $|\log_2FC| > 1$ by “limma” R package). Among these genes, *ALKBH5*, *METTL14*, *YTHDC1*, *YTHDC2*, *YTHDF2*, *YTHDF3*, *ZC3H13*, and *FTO* were lowly expressed in LUSC, while *HNRNPA2B1*, *HNRNPC*, *IGF2BP1*, *IGF2BP2*, *IGF2BP3* and *ALKBH5* were highly expressed (see [Figure S2](#)). In the Spearman

correlation analysis, *METTL3* “writers” were negatively correlated with *FTO* “erasers” ($R = -0.17$ and $P < 0.0001$ by cBioportal for Cancer Genomics); however, this was not the case in LUAD ($R = 0.57$ and $P > 0.05$).

In relation to the prognostic genes, the expression of 14 m6A RNA methylation regulators of differential expression were analyzed by a univariate Cox regression analysis. However, no gene was found to be related to prognosis. *FTO* had the lowest P value. Thus, we theorized that *FTO*, a demethylase for m6A modification, was significantly correlated with prognosis, which was a potential prognostic gene [$P = 0.069$ and hazard ratio (HR) > 1]. According to previous studies, *FTO*, a m6A demethylase, facilitates the progression of lung cancer cells by regulating the m6A level of *USP7* mRNA (14). Additionally, it promotes tumor growth in LUSC by regulating *MZF1* expression (15). These findings suggest that *FTO* is a potential biomarker of LUSC.

Correlation between expression, mutation, and CNVs

As few patients had somatic mutations (see [Table S1](#)), none of the genes with mutations were associated with gene expression. Based on the CNVs in LUSC, *METTL3* was detected to be a significant amplification gene (see [Figure 2A](#)). A Wilcoxon rank-sum test showed that the gains of CNV prompts *METTL3* high expression ($P < 0.01$) (see [Figure 2B](#)). *METTL3* (the RNA modification enzyme methyltransferase-like 3) promotes tumorigenesis and metastasis in oral squamous cell carcinoma, and high *METTL3* expression is related to poor prognosis (16). The results revealed that the expression of *METTL3* mRNA was positively correlated with CNVs. However, recent studies suggest that *METTL3* promotes breast cancer cell proliferation *in vitro* (17). In summary, the gain of CNV might up-regulate high *METTL3* expression in LUSC compared with LUAD (see [Figure S3](#)).

PPI network analysis of FTO and METTL3

Based on the STRING (functional protein association networks) it was predicted that 20 m6A methylation regulators would directly interact with *FTO* and *METTL3* with cutoff: a minimum required interaction score, high confidence (0.70) on-line analysis (string-db.org). The PPI networks of related proteins showed that the *METTL3* gene had internal interactions with “writers”, including *KIAA1429*, *METTL14*, *METTL3*, *RBM15*, *WTAP*,

Table 1 Clinical characteristics in patients on training cohort and validation cohort in this research

Variables	TCGA-LUSC (n=504), n (%)	GSE157010 (n=235), n (%)	GSE157009 (n=249), n (%)	TCGA-LUAD (n=515), n (%)
Age (years)				
60	387 (76.79)	34 (14.47)	37 (14.86)	157 (30.48)
≤60	108 (21.43)	201 (85.53)	212 (85.14)	339 (65.83)
Missing [#]	9 (1.79)			19 (3.69)
Gender				
Male	373 (74.01)	153 (65.11)	161 (64.66)	239 (46.41)
Female	131 (25.99)	82 (34.89)	88 (35.34)	276 (53.59)
TNM stage				
Stage I/II	408 (80.95)	204 (86.81)	231 (92.77)	397 (77.09)
Stage III/IV	92 (18.25)	31 (13.19)	18 (7.23)	110 (21.36)
Missing [#]	4 (0.79)			8 (1.55)
M status				
M0	414 (82.14)			345 (66.99)
M1	7 (1.39)			166 (32.23)
Missing [#]	83 (16.47)			4 (0.78)
N status				
N0	320 (63.49)			332 (64.47)
N1–N3	178 (35.32)			171 (33.20)
Missing [#]	6 (1.19)			12 (2.33)
T status				
T1–T2	409 (81.15)			446 (86.60)
T3–T4	95 (18.85)			69 (13.40)
Smoking grade				
Grade 1–2	152 (30.16)			195 (37.86)
Grade 3–5	340 (67.46)			306 (59.42)
Missing [#]	12 (2.38)			14 (2.72)

[#], ambiguous variables (missing) was excluded. The clinical features of GSE157010 and GSE157009 were not entire like TCGA database, missing M status, N status, T status and smoking grade. TCGA, The Cancer Genome Atlas; LUSC, lung squamous cell carcinoma; LUAD, lung adenocarcinoma; TNM, tumor node metastasis.

and *ZC3H13*, “readers”, including *HNRNPC*, *RBMX*, *HNRNPA2B1*, *YTHDC1*, *YTHDC2*, *YTHDF1*, *YTHDF2*, *YTHDF3*, *FMRI*, and *IGF2BP2*, and “erasers”, including *ALKBH5*, and *FTO* (see *Figure 3*). Additionally, “writers”, “readers” and “erasers”, particularly *FTO* and *METTL3*, had external interactions with each other. We found that *METTL3* was strongly associated with *KIAA1429*, which suggests that *METTL3* has the same function as

KIAA1429.

Confirmed the prognostic model

We compared association with OS as well as accuracy of models with different gene combinations in training cohort, The risk score of *FTO* and *METTL3* was stronger associated with OS than *FTO* and *KIAA1429* (P=0.0023 and P=0.012,

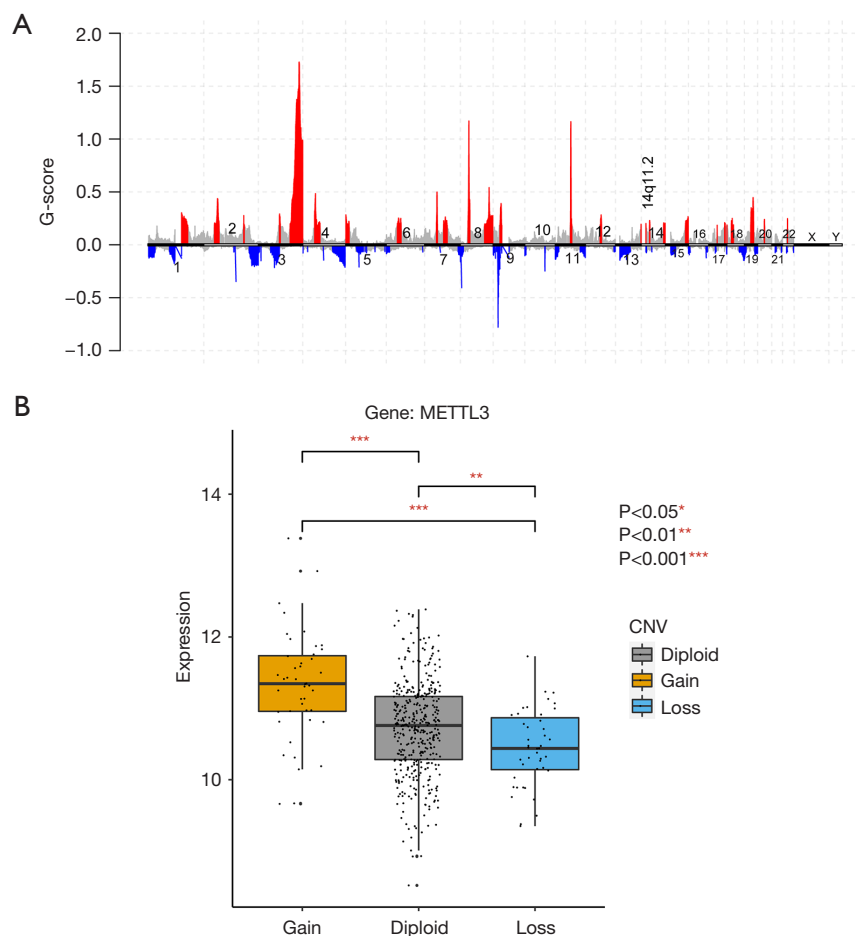


Figure 2 The profile of CNVs and the relationship between the CNV genes and the expression of the m6A-related gene, *METTL3*. (A) The profiles of CNVs in LUSC carcinoma. 14q.11.2 was detected in the chromosome 14 with RNA methylation regulators *METTL3* in it. G-scores assigned by GISTIC for every cytoband plotted along the chromosome. (B) The significant relationship between CNVs and the expression of the m6A-related gene *METTL3* ($P<0.01$). The Y-axis represents expression. CNV, copy number variant; m6A, N6-methyladenosine; LUSC, lung squamous cell carcinoma.

respectively), and the AUC was also higher than *FTO* and *KIAA1429* (3- and 5-year AUC =0.627, 0.653; AUC =0.530,0.547, respectively) (see *Figure 4A-4D*). *FTO* and *METTL3* were selected as the optimal combination. After confirming the model, we verified these results in validation cohort I, showing the integrated model of *FTO* and *METTL3* was an optimum selection. The results showed that high-risk patients [median OS (mOS): 47.7 months] had shorter OS than low-risk patients (mOS: 72.0 months; $P=0.019$). The 3- and 5-year OS AUCs were 0.602 and 0.603, respectively (see *Figure 4E,4F*). To confirm the model in an independent verification, validation cohort II (249 patients) was considered into the two-gene model, the consequence presented the low-risk group [mOS: 85.9 months] has longer OS than high-risk

group (mOS: 61.5 months; $P=0.41$) (see *Table 2*).

Risk score as an independent prognostic indicator

Risk score was calculated to determine whether or not was an independent prognostic indicator of LUSC. Clinicopathological features including, age, gender, TNM stage, M status, T status, N status and smoking grade, and risk score, were analyzed using a univariate Cox hazard regression analysis. The results indicated that TNM stage, smoking grade, and risk score were significantly correlated with OS. Additionally, the results of the multivariate Cox hazard regression revealed that some potential prognostic factors, including smoking

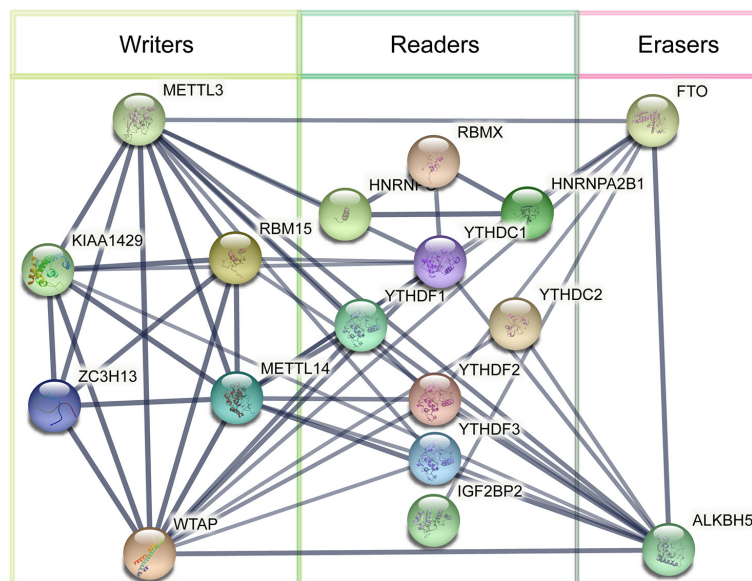


Figure 3 PPI network analysis of the 20 m6A methylation regulators. PPI networks of the related proteins of 20 regulators. “Writers” such as *KIAA1429*, *METTL14*, *METTL3*, *RBM15*, *WTAP*, and *ZC3H13*. “Readers” such as *HNRNPC*, *RBMX*, *HNRNPA2B1*, *YTHDC1*, *YTHDC2*, *YTHDF1*, *YTHDF2*, *YTHDF3*, *FMRI* and *IGF2BP2*. “Erasers” such as *ALKBH5* and *FTO*. Minimum required interaction score: high confidence (0.70). PPI, protein-protein interaction; m6A, N6-methyladenosine.

grade [HR: 1.634; 95% confidence interval (CI): 1.038–2.572; $P=0.00098$] and risk score [HR: 1.699; 95% CI: 1.240–2.3309; $P=0.0014$] were independent prognostic factors of OS (see *Table 3*). Thus, the two-gene model of *FTO* and *METTL3* was an independent prognostic risk-score model of OS.

Association to clinical characteristics with OS

To increase the overall accuracy, survival analysis was performed on clinical characteristics including age, gender, TNM stage, M status, and T status, N status and smoking grade. Kaplan-Meier plot presented TNM, M status, T status, and smoking grade were strong association with OS ($P=0.02$; $P=0.017$; $P=0.0098$; $P=0.0072$, respectively) (see *Figure S4*). Therefore, we constructed a Cox proportional hazards regression model based on risk factors including TNM stage, T status, M status, smoking grade and risk score, and forest plot was drawn to reveal that smoking grade and risk score were significantly higher than other risk factors ($P<0.001$; $P=0.004$, respectively) and concordance index (C-index) was 0.6 in internal verification (see *Figure 5*). Additional, the risk score showed stronger prediction OS in Stage TNM I than other stages ($P=0.0011$) (see *Figure S5*), that means it will

be one of the ways to assess early prognosis.

Relation between risk score and early diagnosis

According to the consequence above, we investigated risk score was associated with early diagnosis. The samples were divided into two groups (normal group and tumor group) in TCGA-LUSC, and *t*-test on risk score of two groups showed quite significant in two groups ($P<2.22e-16$) (see *Figure 6A*). Moreover, the logistic regression model was applied to distinguish patients from healthy persons. The AUC was 0.856, meaning strong detection capabilities in diagnosis (see *Figure 6B*). In a word, this two-gene model can be used as potential markers on both early diagnostic basis and prognostic assessment.

Prognostic nomogram construction

Using a Cox regression model, a prognostic nomogram for 3- and 5-year OS was constructed (see *Figure 7*). A score was assigned to each score level for each influencing factor (e.g., TNM stage, T status, N status, M status, smoking grade, and risk score) according to the contribution degree of each influencing factor in the model in relation to the outcome variable (the size of the regression coefficient), and a total score was then obtained by summing each score.

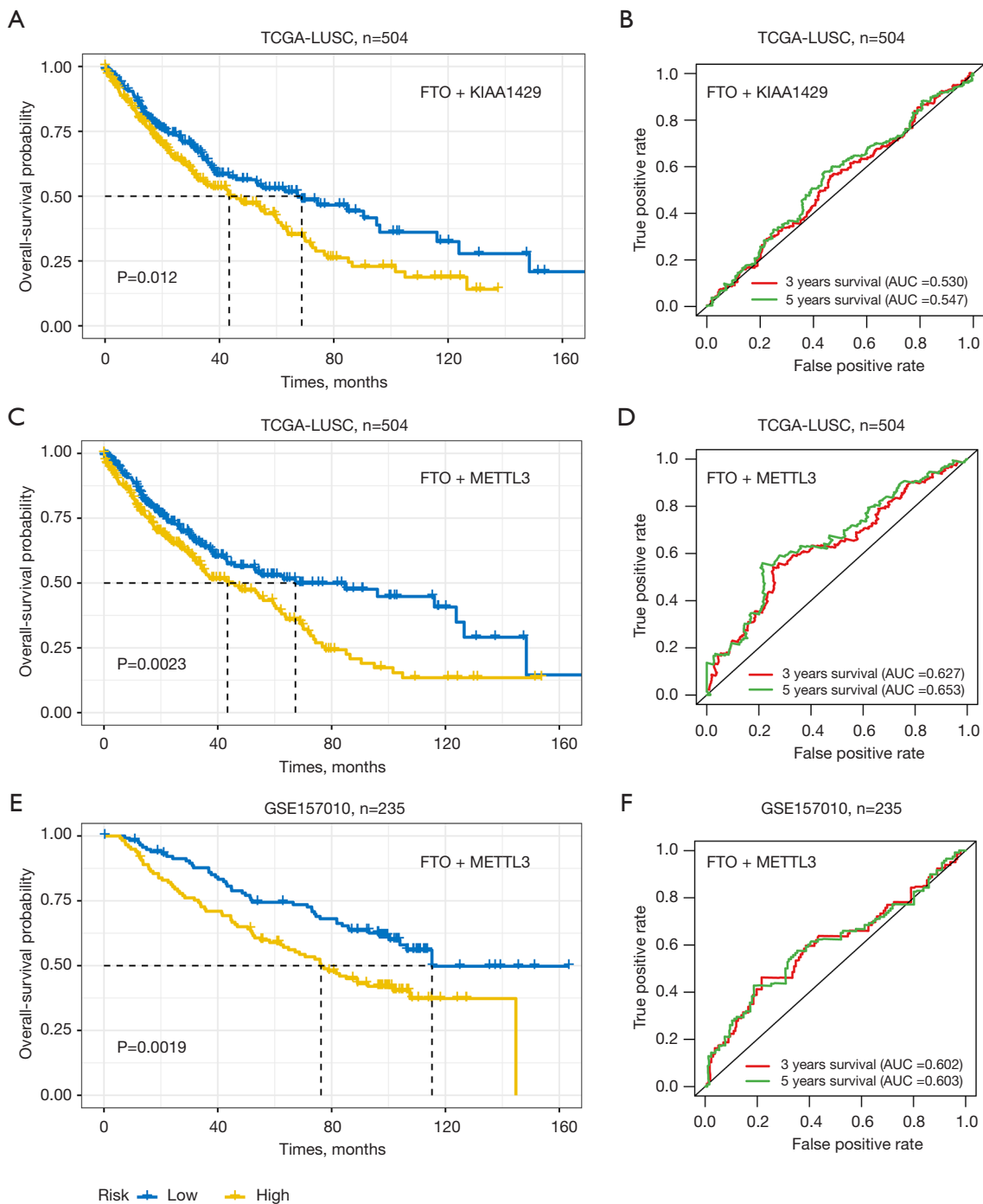


Figure 4 Survival and Accuracy analysis. Kaplan-Meier curve plots for prognostic models and comparison of the sensitivity and specificity of the prediction of OS based on the risk score and other clinical parameters. (A) *FTO* and *KIAA1429* model in TCGA-LUSC (mOS: 68.8 vs. 43.4 months); (B) *FTO* and *KIAA1429* model in TCGA-LUSC (AUC of 3- and 5-year survival: 0.530, 0.547); (C) *FTO* and *METTL3* model in TCGA-LUSC (mOS: 67.3 vs. 43.4 months); (D) *FTO* and *METTL3* model in TCGA-LUSC (AUC of 3- and 5-year survival: 0.627, 0.653); (E) *FTO* and *METTL3* model in GSE157010 (mOS: 72.0 vs. 47.7 months); (F) *FTO* and *METTL3* model in GSE157010 (AUC of 3- and 5-year survival: 0.603, 0.603). Cutoff: $P < 0.05$. TCGA, The Cancer Genome Atlas; LUSC, lung squamous cell carcinoma; mOS, median overall survival; AUC, area under the curve; OS, overall survival.

Table 2 Comparison of different potential biomarkers including the results survival analysis and accuracy analysis

Potential biomarkers	Number	Events	Median (months)	0.95 LCL	0.95 UCL	P value	AUC	
							3-year	5-year
<i>FTO + KIAA1429</i> (TCGA-LUSC)						0.012	0.530	0.547
Low group	247	92	68.8	45.9	96.1			
High group	248	120	43.4	32.3	60.5			
<i>FTO + METTL3</i> (TCGA-LUSC)						0.0023	0.627	0.653
Low group	246	88	67.3	43.4	NA			
High group	249	124	43.4	34.1	60.5			
<i>FTO + METTL3</i> (GEO-GSE157010)						0.0019	0.602	0.603
Low group	117	43	72.0	65.0	NA			
High group	118	69	47.7	38.8	67.2			
<i>FTO + METTL3</i> (GEO-GSE157009)						0.41	0.464	0.459
Low group	124	75	85.9	63.9	102.0			
High group	125	73	61.5	49.2	84.7			
<i>FTO + METTL3</i> (TCGA-LUAD)						0.0479	0.56	0.54
Low group	255	76	58.4	49.2	88.1			
High group	253	107	41.7	36.6	50.3			

Cutoff: $P < 0.05$. LCL, lower confidence limit; UCL, upper confidence limit; AUC, area under the curve; TCGA, The Cancer Genome Atlas; LUSC, lung squamous cell carcinoma; GEO, Gene Expression Omnibus; LUAD, lung adenocarcinoma; CI, confidence interval.

Table 3 Univariate and multivariate Cox regression analysis of the clinicopathological features and potential models in this study

Variables	Patients (n=504), n (%)	Univariate analysis		Multivariate analysis	
		HR (95% CI)	P value	HR (95% CI)	P value
Age (years)		1.25 (0.881–1.791)	0.207		
60	387 (76.79)				
≤60	108 (21.43)				
Missing [#]	9 (1.79)				
Gender		1.197 (0.871–1.644)	0.266		
Male	373 (74.01)				
Female	131 (25.99)				
TNM stage		1.560 (1.135–2.143)	0.006**	1.237 (0.780–1.964)	0.366
Stage I/II	408 (80.95)				
Stage III/IV	92 (18.25)				
Missing [#]	4 (0.79)				

Table 3 (continued)

Table 3 (continued)

Variables	Patients (n=504), n (%)	Univariate analysis		Multivariate analysis	
		HR (95% CI)	P value	HR (95% CI)	P value
M status		3.065 (1.253–7.500)	0.014*	2.316 (0.886–6.054)	0.086
M0	414 (82.14)				
M1	7 (1.39)				
Missing [#]	83 (16.47)				
N status		1.151 (0.872–1.520)	0.318		
N0	320 (63.49)				
N1–N3	178 (35.32)				
Missing [#]	6 (1.19)				
T status		1.648 (1.196–2.270)	0.0022**	1.369 (0.858–2.182)	0.1872
T1–T2	409 (81.15)				
T3–T4	95 (18.85)				
Smoking grade		1.540 (1.161–2.042)	0.0027**	1.699 (1.240–2.3309)	0.00098**
Grade 1–2	152 (30.16)				
Grade 3–5	340 (67.46)				
Missing [#]	12 (2.38)				
FTO (eraser)		1.175 (0.986–1.400)	0.069		
Low	252 (50.00)				
High	252 (50.00)				
FTO (CNV)		0.783 (0.464–1.321)	0.359		
Loss	15 (50.00)				
Gain	18 (50.00)				
METTL3 (writer)		0.932 (0.769–1.130)	0.477		
Low	252 (50.00)				
High	252 (50.00)				
METTL3 (CNV)		0.917 (0.663–1.268)	0.601		
Loss	43 (50.00)				
Gain	44 (50.00)				
KIAA1429 (writers)		1.177 (0.970–1.426)	0.098		
Low	249 (50.30)				
High	246 (49.70)				
Two-gene model (FTO + METTL)		1.44 (1.095–1.891)	0.0089**	1.634 (1.038–2.572)	0.0014**
Low	246 (48.81)				
High	249 (49.40)				

[#], ambiguous variables (missing) were excluded. *, P<0.05; **, P<0.01. HR, hazard ratio; CI, confidence interval; TNM, tumor, node and metastasis; CNV, copy number variant.

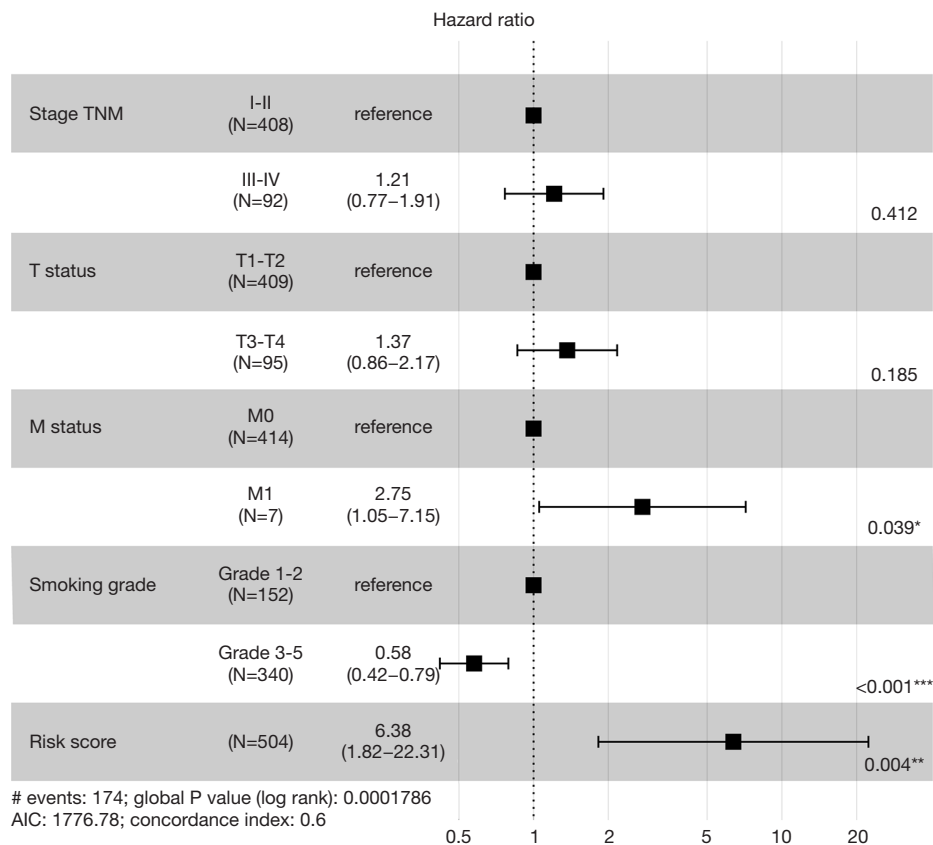


Figure 5 Forest plot for risk factors in LUSC, showing HR and 95% CI. The squares and horizontal lines points out variable HR and 95% CI. Smoking grade and risk score were proved to be independent prognostic factors ($P < 0.001$ and $P = 0.004$, respectively). The log rank test was performed to compare risk factors ($P < 0.001$), and C-index was 0.6. #, summary of Cox regression model; *, $P < 0.05$; **, $P < 0.01$; ***, $P < 0.001$. HR, hazard ratio; CI, confidence interval; C-index, concordance index; AIC, Akaike information criterion.

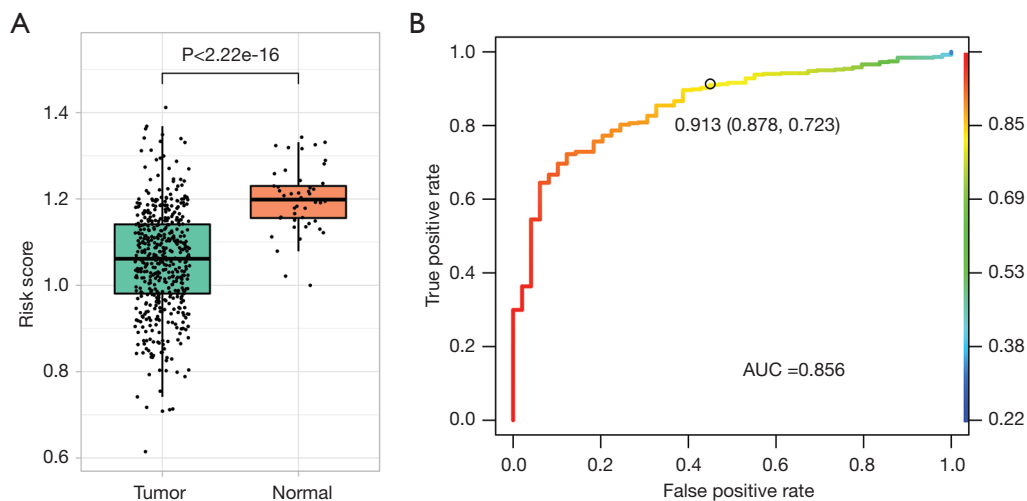


Figure 6 Correlation between risk score and diagnosis. (A) *T*-test was performed to test the significance between normal groups ($n = 49$) and tumor groups ($n = 504$) ($P < 2.22e-16$); (B) AUC was calculated on the diagnostic model (AUC = 0.856). AUC, area under the curve.

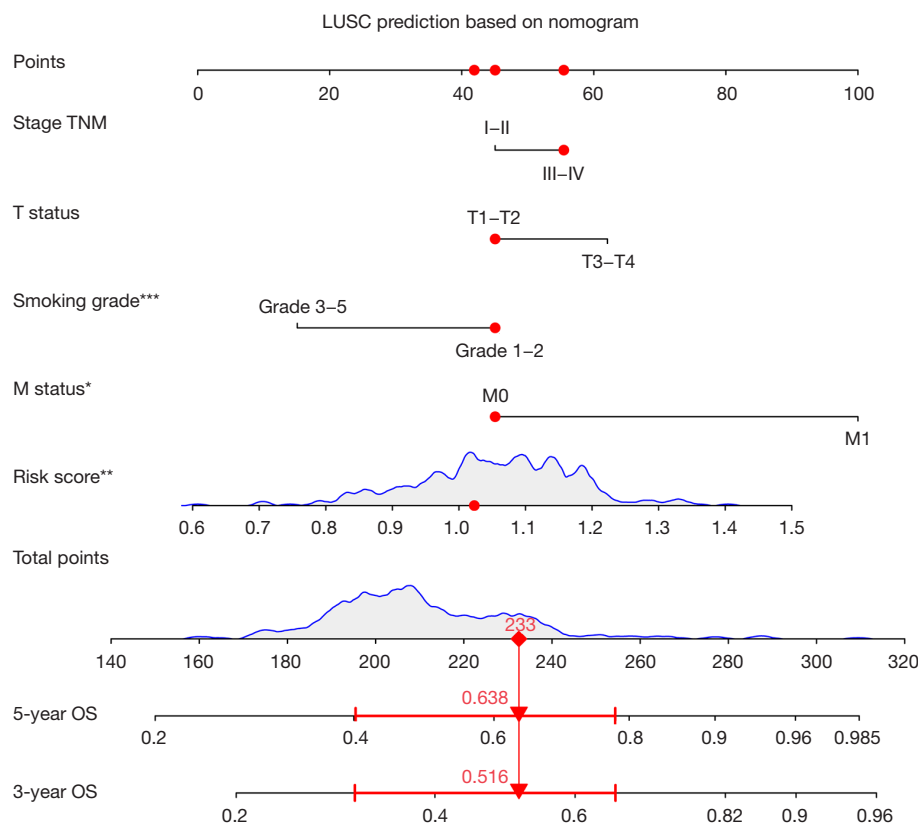


Figure 7 The performance of the nomogram in facilitating clinicians to predict 3- and 5-year OS. Sum of each score for the risk variables, including risk scores and clinicopathological characters, to predict OS. HR (95% CIs). The red dots represent each score for the risk factors, and the red vertical lines represent the total points, which predict the 3- and 5-year survival probability of 1 patient using the LUSC prognosis-based nomogram. *, $P < 0.05$; **, $P < 0.01$; ***, $P < 0.001$. OS, overall survival; HR, hazard ratio; CI, confidence interval; LUSC, lung squamous cell carcinoma; TNM, tumor, node and metastasis.

Finally, the predicted value of an individual's outcome event was calculated by the function transformation between the total score and the probability of the occurrence of the outcome event. This prognostic nomogram is a potentially valuable tool that can help clinicians make individualized treatment decisions.

Discussion

Recently, m6A RNA methylation has become a popular epigenetic regulation topic that has been studied in multiple cancers, such as melanoma, leukemia, prostate, breast cancer, and lung cancer (18-20). m6A RNA methylation modification has been clearly shown to be involved in multiple cellular processes, such as the regulation of mRNA methylation and demethylation. However, a prognostic value (i.e., a risk score), which enables clinicians to predict

the outcome of LUAD, could not be applied to LUSC. Thus, we investigated potential prognostic biomarkers by mining data from public databases.

In our study, we used two public databases (i.e., the TCGA for LUSC and the GEO for GSE157010 and GSE157009) to create training and validation cohorts. The differential expression of 1 of the 20 mRNA methylation regulators (i.e., *FTO*) was analyzed and identified by a univariate Cox regression analysis of 504 tumors paired with normal samples. *METTL3* was recruited because of the significant correlation between expression and CNVs. Then, a two-gene model for *FTO* and *METTL3* was constructed as a prognostic prediction model using the regression coefficients and based on a minimum criteria. The coefficients of the two selected m6A RNA methylation regulators were 0.162 and -0.069. Based on the correlations of 14 DEGs and "writers" and "erasers", *FTO* was found to

be negatively correlated with *METTL3*. These two selected m6A RNA methylation regulators have been previously reported in multiple cancers.

Single-nucleotide polymorphisms (SNPs) in *FTO* was identified and not associated with body mass index (BMI), but was associated with melanoma risk in the first report in 2013 (21). However, it has been reported that rs9939609 polymorphism in the *FTO* gene is associated with a risk of breast and prostate cancer (22). Both genetic changes and *FTO* expression are thought to be involved in the biological process of cancer. As a m6A RNA demethylase, *FTO* plays a role in carcinogenesis, and its high expression promotes leukemic oncogene-mediated cell transformation and leukemogenesis in acute myeloid leukemia, and promotes cell proliferation and migration in esophageal squamous cell carcinoma via the upregulation of *MMP13* (23-25). Similarly, *FTO* expression is associated with the occurrence and prognosis of gastric cancer and papillary thyroid carcinoma (26). In addition, the regulatory factor of m6A RNA methylation has been shown to promote the malignant progression of LUAD and has clinical diagnostic, progressive and prognostic properties (7,8). *FTO* induces *NELL2* expression, which leads to the metastasis of non-small cell lung cancer via the inhibition of *E2F1* m6A modification (27,28) and regulates melanoma tumorigenicity and response to anti-PD-1 blockade (29). Thus, in our study, *FTO* was identified as a potential prognostic biomarker of LUSC.

In recent years, there has been increasing evidences that *METTL3* plays a crucial role in many types of cancers, either independently or dependently of its m6A RNA methyltransferase activity. *METTL3* promotes the translation of m6A methyltransferase in human cancer cells, significantly promotes the progression of hepatocellular carcinoma and breast cancer, and occurs and metastases in oral squamous cell carcinoma and pancreatic cancer cell proliferation and invasion through BMI m6A methylation and pancreatic cancer cell proliferation and invasion (30-32). *METTL3* also acts as a tumor suppressor in renal cell carcinoma (33,34). RNA m6A methyltransferase *METTL3* promotes colorectal cancer by activating the *m6A-GLUT1-mTORC1* axis, and is a therapeutic target. *METTL3* has been recognized as a potential prognostic prediction biomarker in colorectal cancer (35).

Both LUAD and LUSC are non-small cell lung cancers. The biggest difference between LUAD and LUSC is that it is easy to detect early metastasis in LUAD (1,36). For example, even while the lung lesions are relatively small,

there will be brain metastasis, bone metastasis, and even liver metastasis at diagnosis. LUSC can easily lead to the formation of a relatively large mass locally, cause obstructive pneumonia, and is associated with pulmonary hemorrhage and other conditions. However, its rate of growth and metastasis is slow, and it is also sensitive to radiotherapy and chemotherapy. The sensitivity of LUAD to radiotherapy and chemotherapy is worse than that of LUSC, and LUAD is prone to gene mutation, especially epidermal growth factor receptor (*EGFR*) gene mutation. LUAD can be treated with targeted drugs if there is a mutation in the *EGFR* gene. Han *et al.* and Hou *et al.* demonstrate the *de novo* transdifferentiation of lung LUAD to LUSC in mice with *Lkb1* deficiency and provide mechanistic insight that may have important implications for lung cancer treatment (37,38). Previous studies are explored based on expression level analysis and survival analysis, Gene Ontolog analysis and pathway enrichment to reveal the differences and similarities, reporting 4 potential gene markers including *ZWINT*, *A2M*, *POLR2H* and *KIF11* related with miRNA *miR-16-5p* (39-41). Based on variants, both of them have different diver genes, gene fusions. The main driving genes in LUAD are *EGFR* mutation, *ALK* fusion, *ROS-1* fusion, etc., while these in LUSC are *PTEN* mutation, *FGFR1* amplification and 20 common mutated genes including *TP53*, *RB1*, *ARID1A*, *CDKN2A*, *PIK3CA* and *NF1*. Among them, *TP53*, *CDKN2A* and *PIK3CA* mutated more frequently in LUSC than in lung LUAD (42). These differences can lead to different treatment options, such patients could benefit more from nivolumab of immunological therapy in LUSC than LUAD (43). It has been reported in both previous studies and this study that LUSC is strongly linked to smoking (P=0.00098; see *Table 3*), which the mutation rate is about 15% (3). This rate is significantly lower than that of LUAD in China. Those are the main differences between LUAD and LUSC.

The two-gene model is a prognostic score model in LUSC; however, our study had several disadvantages. First, we reached this conclusion using only public databases and bioinformatics. Thus, there is a bias in the model due to the clinical information bias of TCGA-LUSC. As *Table S2* shows, there was no universal rate for 5-year OS in stage I (21.22%); however, a recent report stated that 70% of patients had no metastasis. Additionally, the rate of M0 is 82.14% (414 patients) compared to 1.39% (7 patients) in training cohort. As is well known, clinical information needs to be based on authentic material in clinical research to guarantee the accuracy of the prognostic results. Second, the accuracy of the prognostic risk score of the two-gene

model was not high. Indeed, it was not more than 70% in both the training and validation cohorts, but it appeared robust diagnosis in early patients (AUC =0.856). Therefore, larger samples and independent validations are still required to develop the prognostic biomarkers in future studies.

Thus, the regulatory mechanism of m6A modification in LUSC and LUAD is quite unclear in terms of its biology and pathology processes, and further research in laboratory and clinical settings is required.

Acknowledgments

Funding: None.

Footnote

Reporting Checklist: The authors have completed the TRIPOD reporting checklist. Available at <https://dx.doi.org/10.21037/atm-21-4470>

Conflicts of Interest: All authors have completed the ICMJE uniform disclosure form (available at <https://dx.doi.org/10.21037/atm-21-4470>). HZ and SL are from Chosen Med Technology (Beijing) Co., Ltd., Beijing, China. The other authors have no conflicts of interest to declare.

Ethical Statement: The authors are accountable for all aspects of the work, including ensuring that any questions related to the accuracy or integrity of any part of the work have been appropriately investigated and resolved. The study was conducted in accordance with the Declaration of Helsinki (as revised in 2013). The data released by TCGA database and GEO database are publicly available, and thus informed patient consent was not required.

Open Access Statement: This is an Open Access article distributed in accordance with the Creative Commons Attribution-NonCommercial-NoDerivs 4.0 International License (CC BY-NC-ND 4.0), which permits the non-commercial replication and distribution of the article with the strict proviso that no changes or edits are made and the original work is properly cited (including links to both the formal publication through the relevant DOI and the license). See: <https://creativecommons.org/licenses/by-nc-nd/4.0/>.

References

- Chanvorachote P, Chunhacha P. Chapter 4 - Lung cancer metastasis. In: Ahmad A. editor. Introduction to cancer metastasis. Cambridge: Academic Press, 2017:61-76.
- Bray F, Ferlay J, Soerjomataram I, et al. Global cancer statistics 2018: GLOBOCAN estimates of incidence and mortality worldwide for 36 cancers in 185 countries. *CA Cancer J Clin* 2018;68:394-424.
- Wakelee H, Kelly K, Edelman MJ. 50 years of progress in the systemic therapy of non-small cell lung cancer. *Am Soc Clin Oncol Educ Book* 2014;177-89.
- Fang X, Li M, Yu T, et al. Reversible N6-methyladenosine of RNA: the regulatory mechanisms on gene expression and implications in physiology and pathology. *Genes Dis* 2020;7:585-97.
- Zhou Y, Kong Y, Fan W, et al. Principles of RNA methylation and their implications for biology and medicine. *Biomed Pharmacother* 2020;131:110731.
- Du J, Hou K, Mi S, et al. Malignant evaluation and clinical prognostic values of m6A RNA methylation regulators in glioblastoma. *Front Oncol* 2020;10:208.
- Zhuang Z, Chen L, Mao Y, et al. Diagnostic, progressive and prognostic performance of m6A methylation RNA regulators in lung adenocarcinoma. *Int J Biol Sci* 2020;16:1785-97.
- Li F, Wang H, Huang H, et al. m6A RNA methylation regulators participate in the malignant progression and have clinical prognostic value in lung adenocarcinoma. *Front Genet* 2020;11:994.
- Shi H, Wei J, He C. Where, when, and how: context-dependent functions of RNA methylation writers, readers, and erasers. *Mol Cell* 2019;74:640-50.
- Zhao W, Xie Y. KIAA1429 promotes the progression of lung adenocarcinoma by regulating the m6A level of MUC3A. *Pathol Res Pract* 2021;217:153284.
- Ma L, Chen T, Zhang X, et al. The m6A reader YTHDC2 inhibits lung adenocarcinoma tumorigenesis by suppressing SLC7A11-dependent antioxidant function. *Redox Biol* 2021;38:101801.
- Mendel M, Delaney K, Pandey RR, et al. Splice site m6A methylation prevents binding of U2AF35 to inhibit RNA splicing. *Cell* 2021;184:3125-42.e25.
- Liu GM, Zeng HD, Zhang CY, et al. Identification of METTL3 as an adverse prognostic biomarker in hepatocellular carcinoma. *Dig Dis Sci* 2021;66:1110-26.
- Li J, Han Y, Zhang H, et al. The m6A demethylase FTO promotes the growth of lung cancer cells by regulating the m6A level of USP7 mRNA. *Biochem Biophys Res Commun* 2019;512:479-85.
- Liu J, Ren D, Du Z, et al. m6A demethylase FTO

- facilitates tumor progression in lung squamous cell carcinoma by regulating MZF1 expression. *Biochem Biophys Res Commun* 2018;502:456-64.
16. Liu L, Wu Y, Li Q, et al. METTL3 promotes tumorigenesis and metastasis through BMI1 m6A methylation in oral squamous cell carcinoma. *Mol Ther* 2020;28:2177-90.
 17. Zhang B, Gu Y, Jiang G. Expression and prognostic characteristics of m6A RNA methylation regulators in breast cancer. *Front Genet* 2020;11:604597.
 18. Yi L, Wu G, Guo L, et al. Comprehensive analysis of the PD-L1 and immune infiltrates of m6A RNA methylation regulators in head and neck squamous cell carcinoma. *Mol Ther Nucleic Acids* 2020;21:299-314.
 19. Sun T, Wu R, Ming L. The role of m6A RNA methylation in cancer. *Biomed Pharmacother* 2019;112:108613.
 20. Huang J, Chen Z, Chen X, et al. The role of RNA N6-methyladenosine methyltransferase in cancers. *Mol Ther Nucleic Acids* 2021;23:887-96.
 21. Iles MM, Law MH, Stacey SN, et al. A variant in FTO shows association with melanoma risk not due to BMI. *Nat Genet* 2013;45:428-32, 432e1.
 22. Salgado-Montilla JL, Rodríguez-Cabán JL, Sánchez-García J, et al. Impact of FTO SNPs rs9930506 and rs9939609 in prostate cancer severity in a cohort of Puerto Rican men. *Arch Cancer Res* 2017;5:148.
 23. da Cunha PA, de Carlos Back LK, Sereia AF, et al. Interaction between obesity-related genes, FTO and MC4R, associated to an increase of breast cancer risk. *Mol Biol Rep* 2013;40:6657-64.
 24. Li Z, Weng H, Su R, et al. FTO plays an oncogenic role in acute myeloid leukemia as a N6-methyladenosine RNA demethylase. *Cancer Cell* 2017;31:127-41.
 25. Liu S, Huang M, Chen Z, et al. FTO promotes cell proliferation and migration in esophageal squamous cell carcinoma through up-regulation of MMP13. *Exp Cell Res* 2020;389:111894.
 26. Hou J, Shan H, Zhang Y, et al. m6A RNA methylation regulators have prognostic value in papillary thyroid carcinoma. *Am J Otolaryngol* 2020;41:102547.
 27. Wang Y, Li M, Zhang L, et al. m6A demethylase FTO induces NELL2 expression by inhibiting E2F1 m6A modification leading to metastasis of non-small cell lung cancer. *Mol Ther Oncolytics* 2021;21:367-76.
 28. Zhao T, Wang J, Wu Y, et al. Increased m6A modification of RNA methylation related to the inhibition of demethylase FTO contributes to MEHP-induced Leydig cell injury. *Environ Pollut* 2021;268:115627.
 29. Yang S, Wei J, Cui YH, et al. m6A mRNA demethylase FTO regulates melanoma tumorigenicity and response to anti-PD-1 blockade. *Nat Commun* 2019;10:2782.
 30. Zeng C, Huang W, Li Y, et al. Roles of METTL3 in cancer: mechanisms and therapeutic targeting. *J Hematol Oncol* 2020;13:117.
 31. Xia T, Wu X, Cao M, et al. The RNA m6A methyltransferase METTL3 promotes pancreatic cancer cell proliferation and invasion. *Pathol Res Pract* 2019;215:152666.
 32. Du M, Zhang Y, Mao Y, et al. MiR-33a suppresses proliferation of NSCLC cells via targeting METTL3 mRNA. *Biochem Biophys Res Commun* 2017;482:582-9.
 33. Zhou J, Wang J, Hong B, et al. Gene signatures and prognostic values of m6A regulators in clear cell renal cell carcinoma - a retrospective study using TCGA database. *Aging (Albany NY)* 2019;11:1633-47.
 34. Zhang QJ, Luan JC, Song LB, et al. m6A RNA methylation regulators correlate with malignant progression and have potential predictive values in clear cell renal cell carcinoma. *Exp Cell Res* 2020;392:112015.
 35. Chen H, Gao S, Liu W, et al. RNA N6-methyladenosine methyltransferase METTL3 facilitates colorectal cancer by activating the m6A-GLUT1-mTORC1 axis and is a therapeutic target. *Gastroenterology* 2021;160:1284-300.e16.
 36. Xie S, Wu Z, Qi Y, et al. The metastasizing mechanisms of lung cancer: Recent advances and therapeutic challenges. *Biomed Pharmacother* 2021;138:111450.
 37. Han X, Li F, Fang Z, et al. Transdifferentiation of lung adenocarcinoma in mice with Lkb1 deficiency to squamous cell carcinoma. *Nat Commun* 2014;5:3261.
 38. Hou S, Zhou S, Qin Z, et al. Evidence, mechanism, and clinical relevance of the transdifferentiation from lung adenocarcinoma to squamous cell carcinoma. *Am J Pathol* 2017;187:954-62.
 39. Sun F, Yang X, Jin Y, et al. Bioinformatics analyses of the differences between lung adenocarcinoma and squamous cell carcinoma using The Cancer Genome Atlas expression data. *Mol Med Rep* 2017;16:609-16.
 40. Anusewicz D, Orzechowska M, Bednarek AK. Lung squamous cell carcinoma and lung adenocarcinoma differential gene expression regulation through pathways of Notch, Hedgehog, Wnt, and ErbB signalling. *Sci Rep* 2020;10:21128.
 41. Dong A, Wang ZW, Ni N, et al. Similarity and difference of pathogenesis among lung cancer subtypes suggested by expression profile data. *Pathol Res Pract* 2021;220:153365.

42. Zengin T, Önal-Süzek T. Comprehensive profiling of genomic and transcriptomic differences between risk groups of lung adenocarcinoma and lung squamous cell carcinoma. *J Pers Med* 2021;11:154.
43. Zhang YQ, Yuan Y, Zhang J, et al. Evaluation of the roles

and regulatory mechanisms of PD-1 target molecules in NSCLC progression. *Ann Transl Med* 2021;9:1168.

(English Language Editor: L. Huleatt)

Cite this article as: Zhang K, Han Z, Zhao H, Liu S, Zeng F. An integrated model of *FTO* and *METTL3* expression that predicts prognosis in lung squamous cell carcinoma patients. *Ann Transl Med* 2021;9(20):1523. doi: 10.21037/atm-21-4470

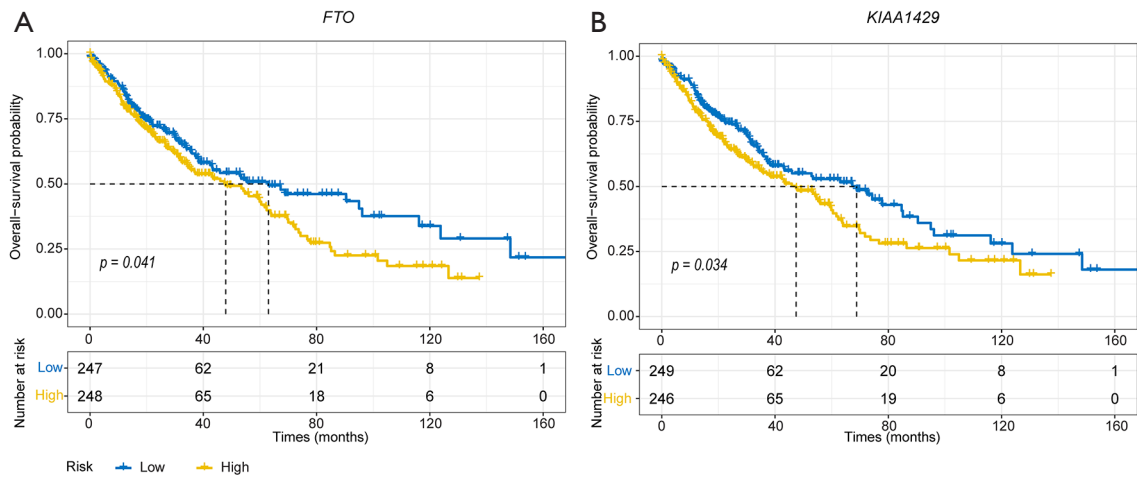


Figure S1 Survival analysis of differential expression m6A regulators. Two of 14 m6A regulators on differential expression were identified to be correlation with OS by Kaplan-Meier plot ($P < 0.05$). (A) *FTO* gene ($P = 0.041$); (B) *KIAA1429* gene ($P = 0.034$); cutoff: $P < 0.05$. m6A, N6-methyladenosine; OS, overall survival.

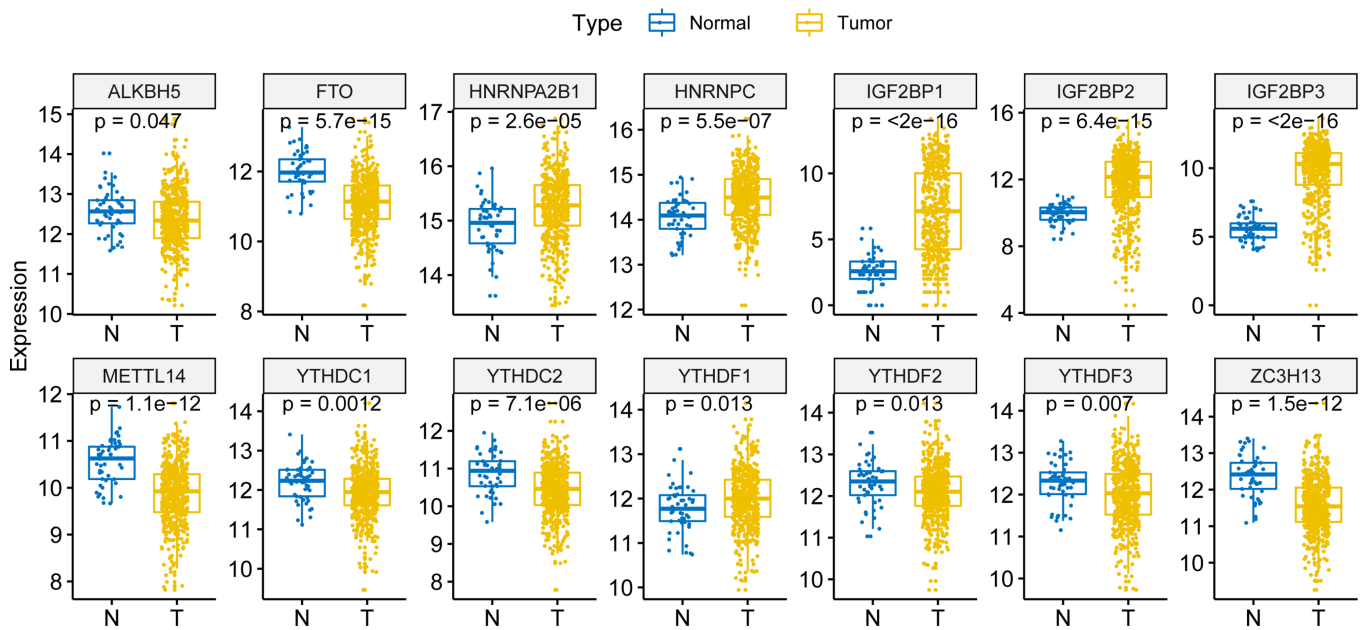


Figure S2 The differential expression levels of 14 m6A RNA methylation regulators between LUSC samples and normal control samples from TCGA-LUSC database ($P < 0.05$). *ALKBH5*, *METTL14*, *YTHDC1*, *YTHDC2*, *YTHDF2*, *YTHDF3*, *ZC3H13* and *FTO* were low expressed in LUSC, *HNRNPA2B1*, *HNRNPC*, *IGF2BP1*, *IGF2BP2*, *IGF2BP3* and *ALKBH5* were high expressed. m6A, N6-methyladenosine; LUSC, lung squamous cell carcinoma; TCGA, The Cancer Genome Atlas.

Table S1 The profile of somatic mutations on LUSC

Sample	<i>FMR1</i>	<i>FTO</i>	<i>HNRNPA2B1</i>	<i>HNRNPC</i>	<i>IGF2BP1</i>	<i>IGF2BP2</i>	<i>METTL14</i>	<i>METTL3</i>	<i>RBM15</i>	<i>RBMX</i>	<i>KIAA1429</i>	<i>WTAP</i>	<i>YTHDC1</i>	<i>YTHDC2</i>	<i>YTHDF1</i>	<i>YTHDF2</i>	<i>YTHDF3</i>	<i>ZC3H13</i>
TCGA-66-2785	P334S										E1664Q							
TCGA-85-6561	R180L																	
TCGA-66-2786	R454P																	
TCGA-66-2789	V621E																	
TCGA-43-2578	V67=																	
TCGA-66-2766		E253Q																
TCGA-18-3407		Q398L																
TCGA-22-5485		S318I								F138S								
TCGA-22-5473			E92Q															
TCGA-33-4566			G237V				D29Y											I327V
TCGA-66-2759				G264W														
TCGA-63-5131				K176N														K821I
TCGA-18-3421					E445*													
TCGA-60-2726					N570K													
TCGA-66-2787					S389I													
TCGA-18-3417						E347K												
TCGA-66-2727						R177Q												
TCGA-37-5819						V111M												
TCGA-85-6560							R21M											
TCGA-60-2708								L172Qfs*10										
TCGA-66-2767									G126R									
TCGA-66-2734									G8V, G8*									
TCGA-34-2600									P300H, M40I									
TCGA-37-3783									R164T									
TCGA-18-4721										I753M								
TCGA-21-1070										K1388*								
TCGA-46-3769										V544L								
TCGA-34-5236										X1547_splice								
TCGA-66-2744											E86K							
TCGA-22-4595											X3_splice							
TCGA-33-6737												D313H						
TCGA-22-4591												R719Q						
TCGA-56-6545													D475Y					
TCGA-18-3419													D820G					
TCGA-66-2763													G18E					
TCGA-66-2756													L1105F					
TCGA-66-2788														R327L				
TCGA-60-2725																R574P		
TCGA-22-1012																		D494G
TCGA-33-4538																		F464L
TCGA-66-2791																		P267L
TCGA-60-2715																		R458Q

*, stop code (nonsense mutation). LUSC, lung squamous cell carcinoma; TCGA, The Cancer Genome Atlas.

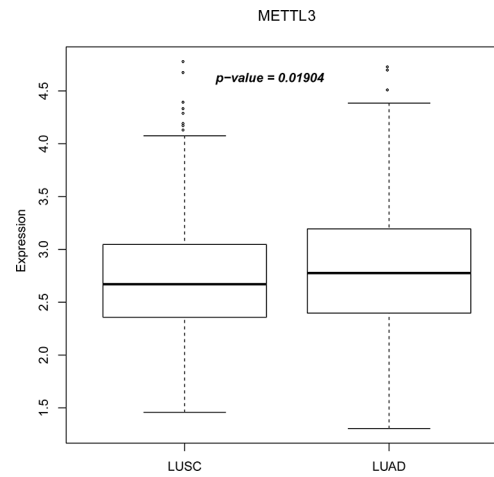


Figure S3 Comparing METTL3 differential expression between LUSC and LUAD. The expression in LUAD was higher than in LUSC by Wilcox test ($P=0.01904$). Y-axis for METTL3 expression. LUSC, lung squamous cell carcinoma; LUAD, lung adenocarcinoma.

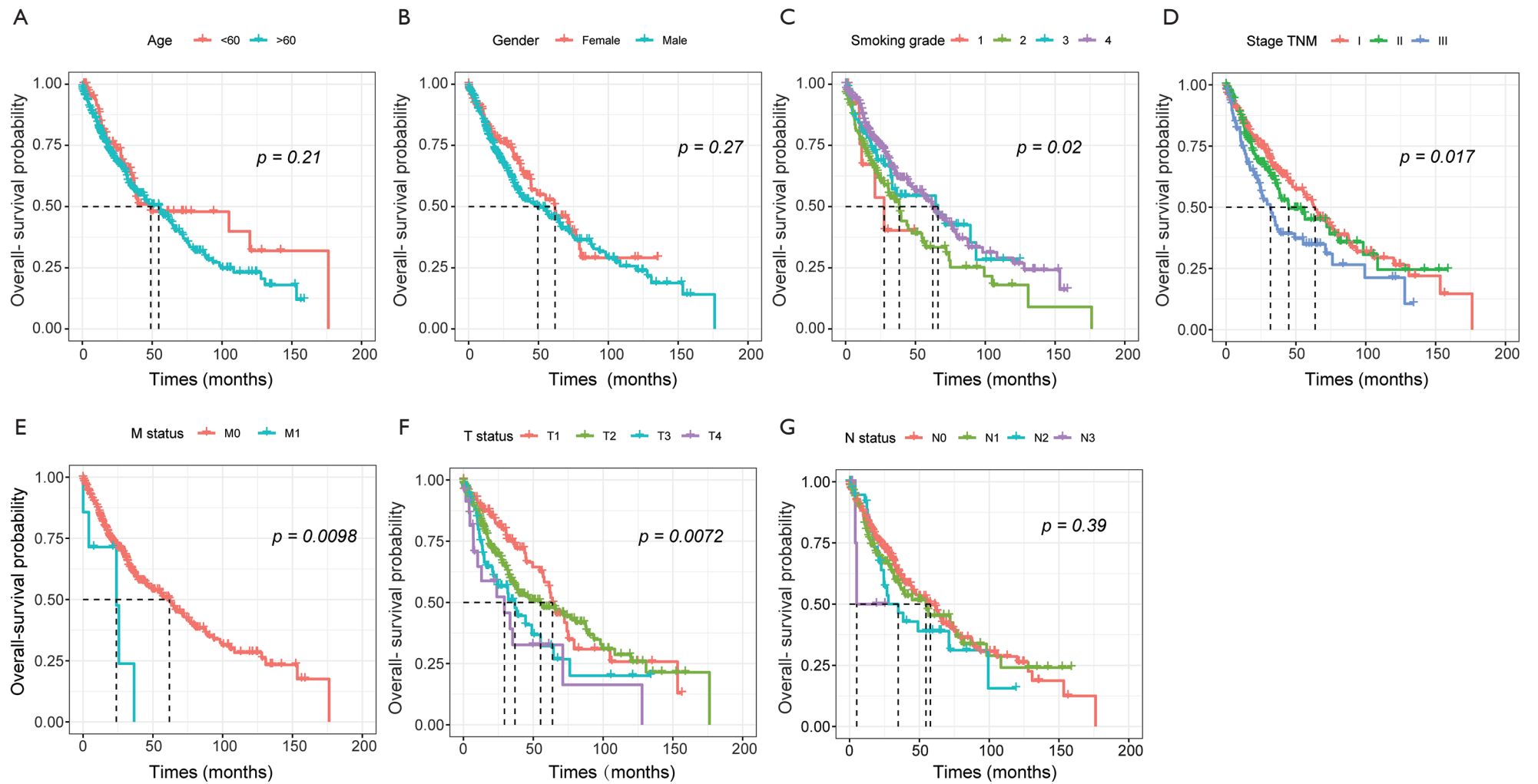


Figure S4 Association to clinical characteristics with OS. Kaplan-Meier plot showed clinical features including smoking grade, stage TNM, M status, T status N status were associated with OS ($P<0.05$). (A) Age ($P=0.21$); (B) gender ($P=0.27$); (C) smoking grade ($P=0.02$); (D) stage TNM ($P=0.017$); (E) M status ($P=0.00098$); (F) T status ($P=0.0072$); (G) N status ($P=0.39$). OS, overall survival; TNM, tumor node metastasis.

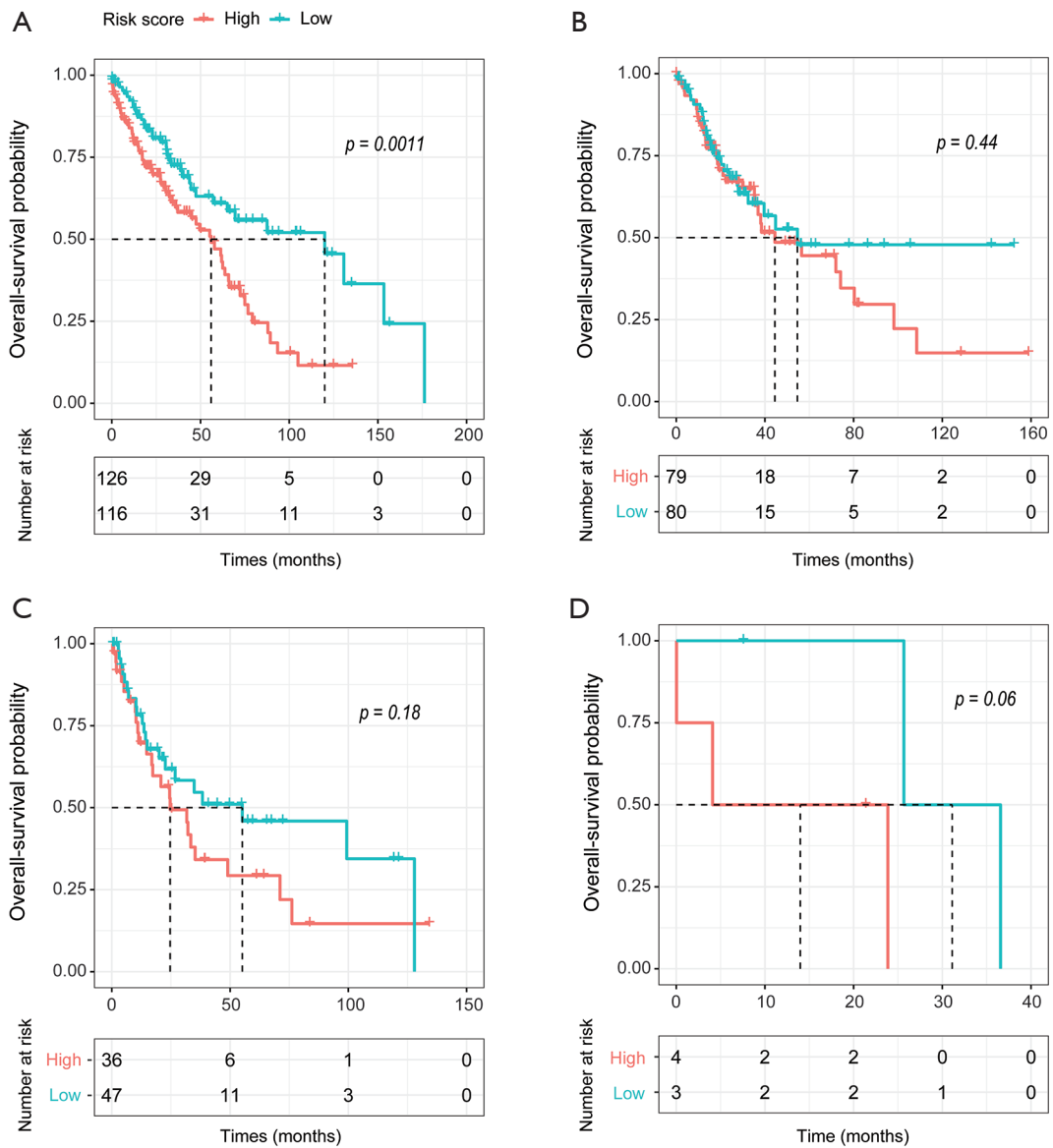


Figure S5 Survival analysis for TNM stage based on risk score. Kaplan-Meier plot illustrates the results in LUSC. (A) Risk score in patients with stage I ($P=0.0011$); (B) stage II ($P=0.44$); (C) stage III ($P=0.18$); (D) stage IV ($P=0.06$). TNM, tumor node metastasis; LUSC, lung squamous cell carcinoma.

Table S2 Comparing percentage of TNM stages with one previously reported

Patients (n=504)	Alive	Dead	Total	Percentage (%)	Percentage previously reported
Stage I				48.6	
Patients	143	102	245		
Patients (>5 years)	31	21	52	21.22	70%
Stage II				32.3	
Patients	97	66	163		
Patients (>5 years)	13	5	18	11.04	
Stage III				16.9	
Patients	40	45	85		
Patients (>5 years)	9	4	13	15.29	
Stage IV				1.4	
Patients	2	5	7		
Patients (>5 years)	0	0	0	0	2%

TNM, tumor, node and metastasis.